contain defects and contamination by amorphous carbon along the length of their walls, which can act as preferential sites for carbonizing to occur.
7. J. Hu, M. Ouyang, P. Yang, C. M. Lieber, *Nature* **399**, 48 (1999).
8. The growth mechanism is inferred from a series of studies of the formation of SiC films on Si substrates, using hydrocarbon or C_{60} carbonization methods that showed that the growth of SiC after nucleation happened at the C/SiC interface rather than the SiC/Si interface [J. Graul and E. Wagner, *Appl. Phys. Lett.* **21**, 67 (1972); C. J. Mogab and H. J. Leamy, *J. Appl. Phys.* **45**, 1075 (1974); J. P. Li and A. J. Steckl, *J. Electrochem. Soc.* **142**, 634 (1995); A. V. Hamza, M. Balooch, M. Moalem, *Surf. Sci.* **317**, L1129 (1994); D. Chen, R. Workman, D. Sarid, *ibid.* **344**, 23 (1995); L. Moro *et al.*, *J. Appl. Phys.* **81**, 6141 (1997); L. Moro *et al.*, *Appl. Surf. Sci.* **119**, 76 (1997)].
9. To prepare the Si specimen, a <111> crystalline Si substrate was thinned by a dimple grinder from a thickness of about 450 μm to several tens of microns at the center. It was further thinned to perforation by chemical etching in a mixed solution with a ratio of $HF:HNO_3$ = 1:4. The thickness near the wedge-shaped perforation edge was less than several tens of nanometers. The oxide film on the Si surface was also removed by the chemical etching. To prepare Ti and Nb specimens, thin foils (thickness ~2 μm) were thinned to perforation by ion milling.
10. The SWCNTs were produced by laser ablation of a graphite target containing 1.2 atomic % of a nickel and cobalt mixture. For a detailed description of the laser ablation method, see (*11*) and T. Guo, P. Nikolaev, A. Thess, D. T. Colbert, R. E. Smalley, *Chem. Phys. Lett.* **243**, 49 (1995).
11. Y. Zhang and S. Iijima, *Philos. Mag. Lett.* **78**, 139 (1998).
12. Strictly speaking, the Si surface as prepared will be terminated by hydrogen or covered with a few monolayers of other surface contaminants, including amorphous carbon, left over from the ethanol used to suspend the SWCNTs. However, these would not influence the result of the experiment, because the surface-terminated hydrogen desorbs at ~500°C [J. Schmidt, M. R. C. Hunt, P. Miao, R. E. Palmer, *Phys. Rev. B* **56**, 9918 (1997)], and the amorphous carbon contamination on the surface of Si forms epitaxial SiC at ~800°C [J. P. Becker, R. G. Long, J. E. Mahan, *J. Vac. Sci. Technol.* **A12**, 174 (1994); R. C. Henderson, R. B. Marcus, W. J. Polito, *J. Appl. Phys.* **42**, 1208 (1971)].
13. A JEM-2000FXVII microscope, with a vacuum of about 10^{-9} torr, was used for the heating experiments and for high-resolution microscopy.
14. The bright spots in the SiC {220} ringlike diffraction pattern indicate a partially epitaxial growth of SiC in a relatively thick Si region. The existence of unreacted Si is also indicated in the same diffraction pattern. The splitting of Si {220} diffraction spots is due to the deformation of the Si substrate during heating.
15. An achiral (10, 10) SWCNT has a diameter close to that indicated by the experimental data. For an explanation of the chiral vector of a nanotube, see (*4*).
16. Bulk self-diffusion parameters for TiC and NbC can be found in G. V. Samsonov and I. M. Vinitskii, *Handbook of Refractory Compounds* (IFI/Plenum, New York, 1980), pp. 222–223.
17. Partially supported by the Special Coordination Funds of the Science and Technology Agency of the Japanese Government. E.L. acknowledges the support of L. D. Marks.

26 April 1999; accepted 20 July 1999

Recognition of the Codon-Anticodon Helix by Ribosomal RNA

Satoko Yoshizawa, Dominique Fourmy, Joseph D. Puglisi*

Translational fidelity is established by ribosomal recognition of the codon-anticodon interaction within the aminoacyl–transfer RNA (tRNA) site (A site) of the ribosome. Experiments are presented that reveal possible contacts between 16*S* ribosomal RNA and the codon-anticodon complex. N1 methylation of adenine at position 1492 (A1492) and A1493 interfered with A-site tRNA binding. Mutation of A1492 and A1493 to guanine or cytosine also impaired A-site tRNA binding. The deleterious effects of A1492G or A1493G (or both) mutations were compensated by 2′fluorine substitutions in the mRNA codon. The results suggest that the ribosome recognizes the codon-anticodon complex by adenine contacts to the messenger RNA backbone and provide a mechanism for molecular discrimination of correct versus incorrect codon-anticodon pairs.

The fidelity of protein synthesis is determined by the interaction of an mRNA codon with the anticodon of the correct (cognate) transfer RNA (tRNA) within the aminoacyl-tRNA site (A site) of the ribosome. The ribosome distinguishes the correct codon-anticodon pair from all noncognate pairs. Despite the relatively low specificity of the codon-anticodon interaction, the measured fidelity of translation is about one error per 10^4 amino acids (*1*). The ribosome achieves high fidelity through a kinetic discrimination mechanism that couples codon-anticodon recognition on the ribosome with hydrolysis of guanosine triphosphate by elongation factor Tu (*2*). Rate constants for tRNA binding to the ribosomal A site are tuned by formation of a cognate or noncognate codon-anticodon pair (*3*). These processes suggest ribosomal recognition of the codon-anticodon pair within an active site for decoding (*4*). The molecular basis of this recognition is not known.

Highly conserved regions of ribosomal RNA (rRNA) form the tRNA-binding sites (*5*). The codon-anticodon interactions in the peptidyl-tRNA site (P site) and A site occur on the small (30*S*) ribosomal subunit (*6*). Fewer nucleotides, located primarily within the 1400 to 1500 region of rRNA, have been implicated in A-site tRNA binding than in P-site tRNA binding (*6*). This agrees with the affinity of a cognate tRNA for the A site being one-fiftieth that for the P site. RNA mutations in 16*S* rRNA affect the fidelity of translation (*5*), and aminoglycoside antibiotics that decrease the fidelity of translation (*7*) bind to 16*S* rRNA and perturb rRNA structure (*8*). These data suggest that the ribosome recognizes the codon-anticodon complex within a defined region of 16*S* rRNA in the 30*S* subunit.

Here, we describe experiments that map possible molecular contacts between 16*S* rRNA and the mRNA-tRNA complex in the A site. Chemical modification interference identified A1492 and A1493 in 16*S* rRNA as required for mRNA-dependent tRNA binding in the A site. Mutations of these two universally conserved nucleotides are lethal in *Escherichia coli* and decrease A-site binding affinity. The deleterious effects of A to G changes at these positions are compensated by 2′F modifications in the mRNA codon. The results support a model for ribosomal decoding in which A1492 and A1493 recognize the helical structure of cognate codon-anticodon complexes in the A site.

A selection scheme was developed to identify bases in 16*S* rRNA whose chemical modification disrupts A-site tRNA binding (Fig. 1A) (*9*). 3′-biotin-$tRNA^{Phe}$ (biotin-$tRNA^{Phe}$) was directed to the A site by saturating the P site with *E. coli* $tRNA^{fMet}$ at the first two codons of phage T4 gene32 mRNA (*10*). In the absence of $tRNA^{fMet}$, biotin-$tRNA^{Phe}$ binds exclusively to the ribosomal P site in a mRNA-dependent fashion (*11*). A-site or P-site complexes were isolated by means of capture of biotin-$tRNA^{Phe}$ by streptavidin beads (*10*). Specific selection of biotin-$tRNA^{Phe}$ was revealed by toeprint experiments (*12*) on captured 30*S* subunits (Fig. 1, A and B). With saturating concentrations of $tRNA^{fMet}$, only A-site complexes of $tRNA^{Phe}$ were captured; in the absence of $tRNA^{fMet}$, P-site complexes were captured.

The chemical groups in 16*S* rRNA required for high-affinity A-site tRNA binding to 30*S* subunits were identified with this selection scheme. 30*S* subunits that were competent for A-site or P-site biotin-$tRNA^{Phe}$ binding after chemical modification were captured with streptavidin beads (*10*, *13*). Comparison of the modification levels of all bases in 16*S* rRNA in the total population and in the bound fraction of 30*S* subunits revealed critical bases for A-site tRNA binding. Only

Department of Structural Biology, Stanford University School of Medicine, Stanford, CA 94305–5126, USA.

*To whom correspondence should be addressed. E-mail: puglisi@stanford.edu

methylation of A1492 and A1493 N1 positions interfered with tRNA binding at the A site (Fig. 1, C and D). A1492 and A1493 are a subset of the bases protected from chemical probes by A-site tRNA (*6*). A1408 forms an internal loop structure with A1492 and A1493, but N1 modification of A1408 did not interfere with A-site tRNA binding. In the presence of the aminoglycoside antibiotic paromomycin, methylation of G1494 (N7) also interfered with A-site tRNA binding (Fig. 1D); G1494 (N7) is required for paromomycin binding (*8*), indicating coupling of drug and tRNA affinity in the A site. No interference was observed in the 530 loop after modification with different reagents. This conserved loop is likely involved in A-site tRNA binding indirectly (*14*).

To test the functional importance of A1492 and A1493, we expressed rRNA containing mutations at these two positions in *E. coli* (*15*). These changes included A1492G, A1492C, A1493G, A1493C, A1492G-A1493G, and A1492C-A1493C. All mutations at 1492 and 1493 confer lethal phenotypes when expressed in *E. coli*. Change of A1408, which is not universally conserved, to G produces functional ribosomes (*16*). Thus, A1492 and A1493 are essential for ribosome function in vivo.

The effects of 1492 and 1493 mutations on A-site tRNA binding were determined with the selection scheme described above (*17*). Mutant 30*S* subunits were purified as a mixture with wild-type subunits. Changes in P- or A-site tRNA binding affinity for the mutant will change the mutant/wild-type ratio after selection. G1492-G1493 and C1492-C1493 mutations were deleterious to A-site tRNA binding (Fig. 2A) as were single mutations at 1492 and 1493. Mutations at position 1492 decreased only A-site tRNA binding affinity, whereas those at 1493 or double mutations at 1492 and 1493 decreased both A- and P-site binding affinity. The effects on P-site binding were relieved by higher concentrations of P-site tRNA. 30*S* subunits containing a G1492 or G1493 (or both) mutation showed decreased protections at the N1 position of A1408 by A-site tRNA compared with that observed on the wild-type 30*S* subunits (*18*). The results demonstrate decreased affinity for A-site tRNA binding in these mutants.

The modification-interference and mutational data suggest rRNA chemical groups for interaction with the tRNA-mRNA complex in the A site. In the structure of a model RNA oligonucleotide, the N1 positions of A1492 and A1493 point into the minor groove of the RNA (*8*). Methylation of the N1 positions of A1492 and A1493 and mutations to guanine remove a hydrogen bond acceptor, the adenine N1 position. The hydrogen bond donor likely resides in the mRNA. A-site tRNA binding is strictly mRNA dependent (*19*), and the 2′OH groups of the mRNA are important for translation (*20*). Substitution of 2′OH groups with deoxynucleotides in the A-site codon decreases the binding affinity of the cognate tRNA but does not affect P-site tRNA binding (*21*). These data suggest that the 2′OH groups within the codon may interact with rRNA in the A site, possibly through hydrogen bonds to the N1 positions of A1492 and A1493.

Recognition of the codon-anticodon complex through adenine N1-2′OH interactions was tested experimentally by exchange for guanine NH1-2′F interactions (*22*). The energetics of C-F–H-N hydrogen bonds are not known, but crystal structures have demonstrated their formation (*23*). The A-site selection was applied to mixtures of wild-type and two double mutant ribosomes (G1492-G1493 and C1492-C1493) bound to gene32 mRNA containing either 2′OH, 2′H, or 2′F uridines (*24*) (Fig. 2, A and B). The mutant/wild-type ratio reveals the relative effects of rRNA or mRNA changes on A-site binding affinity.

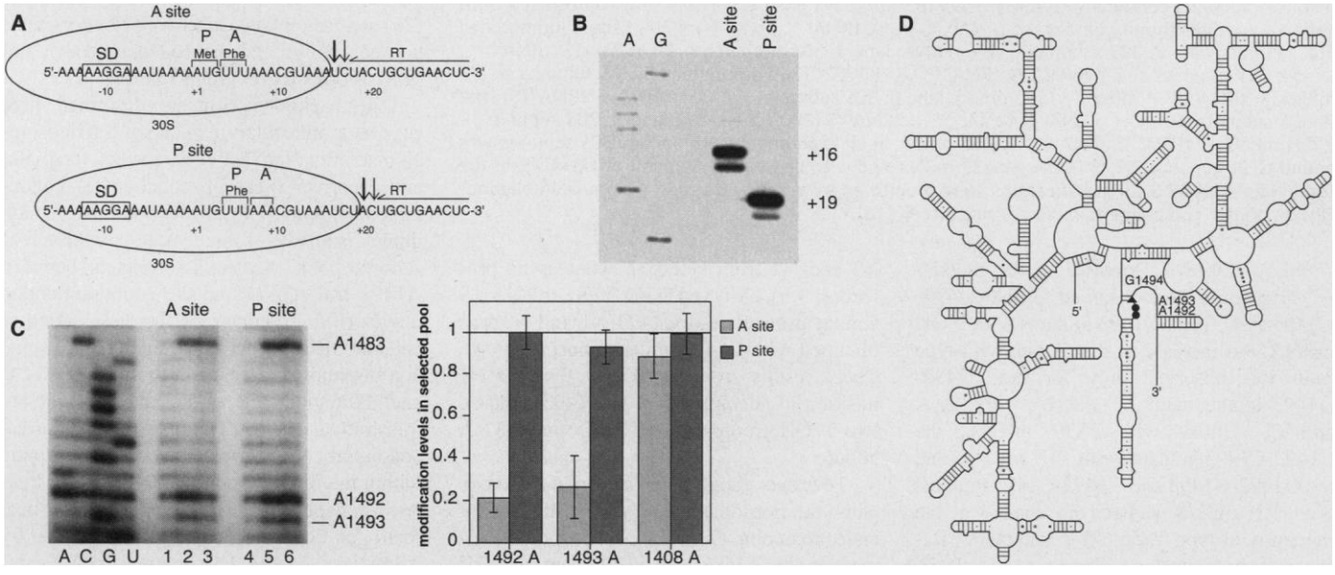

Fig. 1. (**A**) Isolation of chemically modified or mutant 30*S* ribosomal subunits that retain their A-site tRNA-binding activity. Shine-Dalgarno sequence (SD) and codons for methionine (AUG) and phenylalanine (UUU) of T4 phage gene32 mRNA are indicated. Subunits whose binding affinity is not affected are captured with magnetic streptavidin beads, which bind to biotin-tRNA^{Phe}. A-site complexes are formed by addition of tRNA^{fMet} and biotin-tRNA^{Phe}, whereas P-site complexes are formed by addition of only biotin-tRNA^{Phe}. Stops of reverse transcription (RT) caused by 30*S* subunit in the toeprint experiment are indicated by a small and a large arrow. (**B**) Autoradiograph showing the toeprint stops for A-site and P-site complexes after capture with streptavidin beads. With excess tRNA^{fMet} over 30*S* subunits, tRNA^{Phe} binds exclusively to the A site, whereas in the absence of tRNA^{fMet}, it binds to the P site. A and G are dideoxy sequencing lanes. Numbers at right indicate positions on the gene32 mRNA. (**C**) (Left) Base modifications of 16*S* rRNA that interfere with A-site tRNA binding. The autoradiograph shows a region of 16*S* rRNA around position A1483 (control), A1492, and A1493. 30*S* subunits were modified with DMS. Lanes 1 and 4 show primer extension of unmodified 16*S* rRNA, lanes 2 and 5 show the total population of modified 16*S* rRNA, and lanes 3 and 6 show the captured subpopulation of modified 16*S* rRNA. A-site and P-site labels indicate A-site and P-site selection, respectively. The lanes labeled A, C, G, and U are dideoxy sequencing lanes. (Right) The graph shows quantification of interference of A-site tRNA binding by modification of N1 positions of A1492 and A1493. Error bars are derived from at least three independent experiments. (**D**) Secondary structure of 16*S* rRNA showing critical nucleotides for A-site tRNA binding to 30*S* subunits (●). Methylation of G1494 (N7) only interfered with tRNA binding in the presence of 100 μM paromomycin (▲).

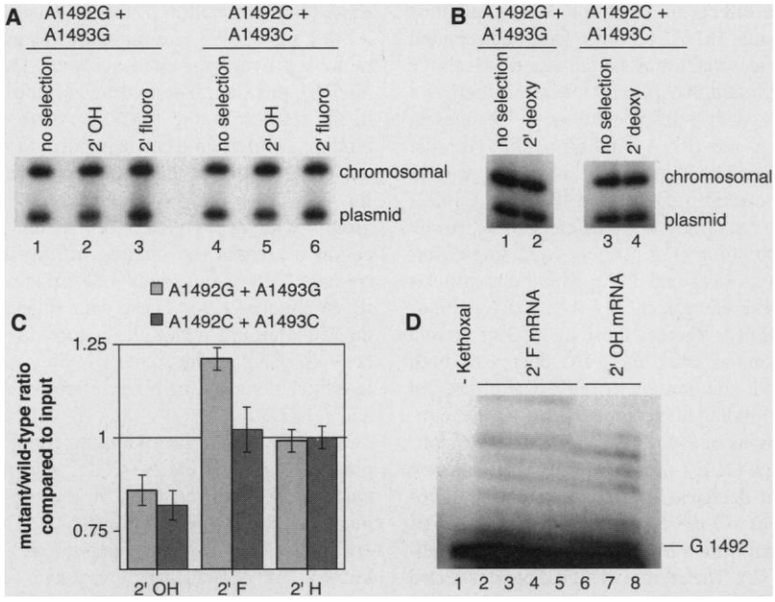

Fig. 2. The A-site selection was applied to mixtures of wild-type and two mutant ribosomes, G1492-G1493 or C1492-C1493 bound to gene32 mRNA containing either 2′OH, 2′F (A), or 2′H uridines (B). **(A)** Lanes 1 and 4 show the ratio of chromosomal and plasmid encoded 16*S* rRNA in the wild-type/mutant 30*S* subunit mixture before A-site selection. Lanes 2 and 5 and 3 and 6 show the 16S rRNA ratio observed with capture of 30*S* subunits with 2′OH or 2′F mRNA, respectively. **(B)** Lanes 1 and 3 show the ratio of the wild-type/mutant 30*S* subunits mixture before A-site selection. Lanes 2 and 4 show the 16*S* rRNA ratio observed with capture of 30*S* subunits with 2′H mRNA. **(C)** Bar graph representing the variations in the mutant/wild-type ratio after selection for A-site binding with mRNA containing either 2′OH, 2′F, or 2′H uridines. Error bars are derived from at least three independent experiments. **(D)** Autoradiograph showing kethoxal probing experiments with 30*S* subunits containing G1492-G1493 mutation. N1 position of G1492 was protected from kethoxal modification by binding of $tRNA^{fMet}$, yeast $tRNA^{Phe}$, and 2′F mRNA. Lane 1, unmodified 30*S* subunits; lane 2, 30*S* subunits + 2′F mRNA; lane 3, 30*S* subunits + 2′F mRNA + $tRNA^{fMet}$; lane 4, 30*S* subunits + 2′F mRNA + $tRNA^{fMet}$ + $tRNA^{Phe}$ (200 pmol); lane 5, 30*S* subunits + 2′F mRNA + $tRNA^{fMet}$ + $tRNA^{Phe}$ (500 pmol); lane 6, 30*S* subunits + 2′OH mRNA + $tRNA^{fMet}$; lane 7, 30*S* subunits + 2′OH mRNA + $tRNA^{fMet}$ + $tRNA^{Phe}$ (200 pmol); and lane 8, 30*S* subunits + 2′OH mRNA + $tRNA^{fMet}$ + $tRNA^{Phe}$ (500 pmol). In all experiments, 10 pmol of 30*S* subunits was bound to 30 pmol of 2′F or 2′OH gene32 mRNA and with or without 50 pmol of $tRNA^{fMet}$ in the total volume of 12.5 μl. Modifications were monitored by primer extension from a DNA oligonucleotide primer complementary to priming site V (*16*).

As shown above, decreases in the mutant/wild-type ratio were observed for the G1492-G1493 and C1492-C1493 mutants with 2′OH mRNA. An increase in the mutant/wild-type ratio was observed only for the G1492-G1493 mutant with 2′F mRNAs (Fig. 2, A and C). Unlike with 2′OH mRNA, the C1492-C1493 mutant with 2′F mRNA and the G1492-G1493 and C1492-C1493 mutants with 2′H mRNA showed no change in the mutant/wild-type ratio after selection. Because these mutations disrupt A-site tRNA binding with the 2′OH mRNA, the results suggest equally deleterious effects of rRNA mutations and mRNA backbone changes on A-site tRNA-binding. 30*S* subunits containing a single G1492 or G1493 mutation gave results similar to those of the G1492-G1493 mutant.

The selection results with mutant ribosomes and 2′F mRNA were confirmed by footprinting. Addition of $tRNA^{fMet}$ and $tRNA^{Phe}$ with 2′F mRNA to G1492 and G1493 mutant ribosomes protected G1492 N1 and N2 from kethoxal, whereas no protection was observed with 2′OH mRNA. A similar protection at G1493 N1 and N2 was obtained with G1493 mutant ribosomes (*18*). These results strongly suggest that the N1 position of adenines 1492 and 1493 contacts two 2′ OH groups of an A-site bound mRNA codon.

To ensure translation of all codon-anticodon pairs, the ribosome should contact the codon-anticodon complex in a sequence-independent manner (*8*). A1492 and A1493 contact 2′OH groups in the mRNA codon, which forms an A-form duplex with a cognate tRNA anticodon; similar recognition of base-pair shape occurs within the active site of DNA polymerase (*25*). The small energetic effects of rRNA and mRNA modifications on A-site tRNA affinity are consistent with the dominant contribution of the codon-anticodon interaction to A-site tRNA binding (*3*). Aminoglycoside antibiotics, which distort the structure of A1492 and A1493 and the surrounding helix (*8*), increase the affinity of A-site tRNAs by favoring contacts between

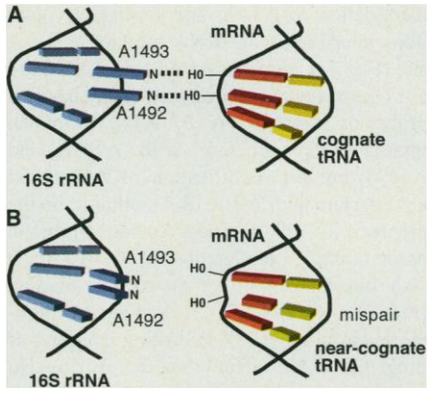

Fig. 3. Schematic model for ribosome mRNA-tRNA interaction in the A site. **(A)** The N1 positions of A1492 and A1493 in 16*S* rRNA can contact two 2′OH in the mRNA codon. The interaction between the cognate tRNA and mRNA places the codon in the proper orientation to interact with the ribosomal A site and leads to efficient conformational signaling. **(B)** The interaction between near-cognate tRNA and mRNA leads to a mispair in the first two positions of the codon-anticodon helix, which distorts its structure, disrupting N1 contacts and decreasing conformational signaling.

the codon-anticodon helix and these nucleotides (*7*). The interactions between rRNA and the codon-anticodon complex are probably more intricate than a pair of hydrogen bonds between A1492 and A1493 and the mRNA backbone (*26*) and may involve a network of interactions between rRNA and the codon-anticodon duplex, as observed in group I introns (*27*).

The backbone contacts described here suggest a molecular mechanism for ribosomal discrimination between correct (cognate) and incorrect (near or noncognate) codon-anticodon pairs. The correct codon-anticodon duplex is a two– or three–base pair stretch of A-form helix. Molecular contacts between A1492 and A1493 and the codon-anticodon duplex (Fig. 3A) decrease the dissociation of cognate tRNA and may trigger additional conformational changes in the 530 loop (*14*) and 900 regions (*28*) of 16*S* rRNA, which are transmitted to the 50*S* subunit (*3*). Incorrect codon-anticodon duplexes contain mispairs within the first two positions that distort their A-form geometry and the positions of critical hydrogen bonding groups for recognition by A1492 and A1493. Disruption of rRNA contacts (Fig. 3B) increases the dissociation rate of incorrect tRNAs and decreases conformational signaling rates (*3*). The ribosome thus distinguishes between different helical structures formed by correct and incorrect codon-anticodon complexes during decoding.

Reference and Notes

1. H. J. Grosjean, S. de Henau, D. M. Crothers, *Proc. Natl. Acad. Sci. U.S.A.* **75**, 610 (1978); C. G. Kurland, *Annu. Rev. Genet.* **26**, 29 (1992).
2. M. V. Rodnina, T. Pape, R. Fricke, L. Kuhn, W. Wintermeyer, *EMBO J.* **14**, 2613 (1995); *J. Biol. Chem.* **271**,

646 (1996); T. Pape, W. Wintermeyer, M. Rodnina, *EMBO J.* **18**, 3800 (1999).
3. T. Pape, W. Wintermeyer, M. V. Rodnina, *EMBO J.* **17**, 7490 (1998).
4. J. Davies, W. Gilbert, L. Gorini, *Proc. Natl. Acad. Sci. U.S.A.* **51**, 883 (1964).
5. R. Green and H. F. Noller, *Annu. Rev. Biochem.* **66**, 679 (1997).
6. D. Moazed and H. F. Noller, *Cell* **47**, 985 (1986); *J. Mol. Biol.* **211**, 135 (1990).
7. D. Moazed and H. F. Noller, *Nature* **327**, 389 (1987); R. Karimi and M. Ehrenberg, *Eur. J. Biochem.* **226**, 355 (1994).
8. D. Fourmy, M. I. Recht, S. C. Blanchard, J. D. Puglisi, *Science* **274**, 1367 (1996); D. Fourmy, S. Yoshizawa, J. D. Puglisi, *J. Mol. Biol.* **277**, 333 (1998); S. Yoshizawa, D. Fourmy, J. D. Puglisi, *EMBO J.* **17**, 6437 (1998); S. C. Blanchard, D. Fourmy, R. G. Eason, J. D. Puglisi, *Biochemistry* **37**, 7716 (1998).
9. U. von Ahsen and H. F. Noller, *Science* **267**, 234 (1995).
10. Biotin was attached to the 3′ end of yeast $tRNA^{Phe}$ (Sigma) as previously described (*9*). The gene32 mRNA fragment corresponding to positions −55 to +85 and *E. coli* ribosomal subunits was prepared with standard methods. Binding of biotin-$tRNA^{Phe}$ to the A site was confirmed by chemical probing of 30*S* subunits (*6*). A-site or P-site biotin-$tRNA^{Phe}$-ribosome complexes were captured by incubation for 20 min at room temperature with magnetic streptavidin beads (streptavidin-M280; Dynal; 12.5 μg of beads per 1 pmol of biotin-$tRNA^{Phe}$). The beads were prewashed three times with buffer containing 0.3% bovine serum albumin (BSA) and once with buffer lacking BSA, and the unbound subunits were removed by washing three times with the 20 μl of binding buffer after the beads were trapped with a magnet.
11. S. Watanabe, *J. Mol. Biol.* **67**, 443 (1972); R. Lill, J. M. Robertson, W. Wintermeyer, *Biochemistry* **25**, 3245 (1986).
12. D. Hartz, D. S. McPheeters, R. Traut, L. Gold, *Methods Enzymol.* **164**, 419 (1988). For toeprinting, gene 32 mRNA was annealed to 5′ ^{32}P–end-labeled primer as described. The A-site complex was formed with 5 pmol of mRNA, 10 pmol of 30*S* subunit, 50 pmol of $tRNA^{fMet}$, and 10 pmol of biotin-$tRNA^{Phe}$ in 12 μl of selection buffer [80 mM potassium cacodylate (pH 7.2), 150 mM NH_4Cl, 1 mM dithiothreitol, and 12 mM $MgCl_2$]. The P-site complex was formed by excluding $tRNA^{fMet}$. The A-site or P-site complex was captured with magnetic streptavidin beads as in (*10*). Primer extension was performed directly on the beads.
13. For modification-interference experiments, 30*S* subunits (320 pmol) were first modified with dimethyl sulfate (DMS), kethoxal, or 1-cyclohexyl-3-(2-morpholinoethyl)carbodiimide metho-*p*-toluenesulfonate at 37°C for 10 min (*6*). Reagents were subsequently removed by spinning with microcon 30 (Amicon). The A-site or P-site complex was formed with 100 pmol of 30*S* subunits, 250 pmol of mRNA, with or without 500 pmol of $tRNA^{fMet}$, and 50 pmol of biotin-$tRNA^{Phe}$ in 20 μl of selection buffer. For selection in the presence of paromomycin, 100 μM drug was added. The active subunits were captured with beads and released by addition of 20 μl of 5 mM EDTA, 0.5% SDS, and 300 mM sodium acetate (pH 5.4) and incubation at room temperature for 20 min. Modifications were detected by primer extension with 12 independent primers to scan the entire sequence of 16*S* rRNA. Modification levels were quantified with a Phosphorimager (Molecular Dynamics), normalized to account for differences in lane loadings, and background levels estimated from unmodified sample lanes were subtracted. Modification of the same set of nucleotides as observed in (*9*) interfered with P-site tRNA binding, except that the interference at G1401 (N7) was not observed.
14. T. Powers and H. F. Noller, *Trends Genet.* **10**, 27 (1994).
15. Oligonucleotide-directed mutations were constructed in pBS-V as described (*16*). Mutations were introduced into an expression plasmid that contains the rrnB operon under control of phage lambda P_L promoter and cI857, a thermolabile allele of the lambda repressor. Strain DH1 was used as the recipient of the final constructs.
16. M. I. Recht, S. Douthwaite, K. D. Dahlquist, J. D. Puglisi, *J. Mol. Biol.* **286**, 33 (1999).
17. The A-site complex was formed by incubating the mixture of mutant 30*S* subunits and wild-type subunits (50 pmol total), 250 pmol of gene32 mRNA, 250 pmol of $tRNA^{fMet}$, and 10 pmol of $tRNA^{Phe}$ in 10 μl of selection buffer. The ratio between mutant and wild-type ribosomal subunit population was analyzed by primer extension from allele-specific priming site V as described (*16*). The mutant population in each mixture was A1492G, 40 ± 3%; A1492C, 40 ± 2%; A1493G, 32 ± 2%; A1493C, 23 ± 3%; A1492G-A1493G, 32 ± 3%; and A1492C-A1493C, 43 ± 2%.
18. S. Yoshizawa and J. D. Puglisi, unpublished results.
19. R. A. Grajevskaja, Y. V. Ivanov, E. M. Saminsky, *Eur. J. Biochem.* **128**, 47 (1982); S. V. Kirillow, E. M. Makarov, Y. Semenkov, *FEBS Lett.* **157**, 91 (1983); R. Lill, J. M. Robertson, W. Wintermeyer, *Biochemistry* **23**, 6710 (1984).
20. B. J. McCarthy and J. J. Holland, *Proc. Natl. Acad. Sci. U.S.A.* **54**, 880 (1965); H. Aurup, A. Siebert, F. Benseler, D. Williams, F. Eckstein, *Nucleic Acids Res.* **22**, 4963 (1994).
21. A. P. Patapov, F. J. Triana-Alonso, K. Nierhaus, *J. Biol. Chem.* **270**, 17680 (1995).
22. A. M. Pyle, F. L. Murphy, T. R. Cech, *Nature* **358**, 123 (1992).
23. K. Brady, A. Wei, D. Ringe, R. H. Abeles, *Biochemistry* **29**, 7600 (1990); T. R. Burke *et al.*, *ibid.* **35**, 15989 (1996); L. H. Takahashi, R. Radhakrishnan, R. E. Rosenfield Jr., E. F. Meyer Jr., D. A. Trainor, *J. Am Chem. Soc.* **111**, 3368 (1989).
24. The 2′ fluoro- and 2′ deoxy-U mRNAs were transcribed with $Tyr^{639} \rightarrow$ Phe mutant T7 RNA polymerase (*29*) with 2′ fluoro uridine triphosphate (UTP) (Amersham) or 2′ deoxy-UTP (Sigma) as substrates.
25. S. Doublié, S. Tabor, A. M. Long, C. C. Richardson, T. Ellenberger, *Nature* **391**, 251 (1998).
26. M. S. VanLoock, T. R. Easterwood, S. C. Harvey, *J. Mol. Biol.* **285**, 2069 (1999).
27. A. A. Szewczak, L. Ortoleva-Donnelly, S. P. Ryder, E. Moncoeur, S. A. Strobel, *Nature Struct. Biol.* **5**, 1037 (1998); G. J. Narlikar and D. Herschlag, *Biochemistry* **37**, 9902 (1998).
28. J. S. Lodmell and A. E. Dahlberg, *Science* **277**, 1262 (1997).
29. R. Sousa and R. Padilla, *EMBO J.* **14**, 4609 (1995).
30. The authors thank H. Noller, S. Joseph, R. Green, M. Recht, K. Dahlquist, and S. Blanchard for assistance and helpful discussions and R. Sousa for the plasmid encoding the $Tyr^{639} \rightarrow$ Phe mutant T7 RNA polymerase gene. Supported by grants from NIH (GM51266), the Packard Foundation, and the Lucille P. Markey Charitable Trust. S.Y. was supported by a grant from the Japan Society for the Promotion of Science. D.F. was supported by a grant from Institut National de la Santé et de la Recherche Médicale.

1 June 1999; accepted 9 August 1999

Activity-Induced Potentiation of Developing Neuromuscular Synapses

Ji-jun Wan and Mu-ming Poo*

Electrical activity plays a critical role in shaping the structure and function of synaptic connections in the nervous system. In *Xenopus* nerve-muscle cultures, a brief burst of action potentials in the presynaptic neuron induced a persistent potentiation of neuromuscular synapses that exhibit immature synaptic functions. Induction of potentiation required an elevation of postsynaptic Ca^{2+} and expression of potentiation appeared to involve an increased probability of transmitter secretion from the presynaptic nerve terminal. Thus, activity-dependent persistent synaptic enhancement may reflect properties characteristic of immature synaptic connections, and bursting activity in developing spinal neurons may promote functional maturation of the neuromuscular synapse.

Electrical activity can induce modifications of synaptic connections in developing and mature nervous systems (*1*). In various parts of the central nervous system, a brief period of repetitive synaptic activity induces a persistent increase or decrease in synaptic efficacy (*2*), known as long-term potentiation (LTP) or long-term depression (LTD). At developing neuromuscular synapses in culture, a form of persistent heterosynaptic depression similar to LTD can be induced by repetitive stimulation of an adjacent neuron coinnervating the same muscle cell (*3*). Persistent depression can also be induced by repetitive activation of postsynaptic acetylcholine (ACh) receptors with iontophoresis of ACh (*4*) or by a brief elevation of postsynaptic Ca^{2+} through release of caged Ca^{2+} (*5*). However, a phenomenon similar to LTP has not been reported in any neuromuscular system. In this work, we have identified conditions under which repetitive activity can induce persistent enhancement of synaptic transmission at developing neuromuscular synapses in a cell culture preparation.

We made simultaneous whole-cell perforated patch recordings from presynaptic spinal neurons and postsynaptic myocytes in 1-day-old *Xenopus* nerve-muscle cultures (*6*). We assayed the synaptic efficacy by measuring the mean amplitude of excitatory postsynaptic currents (EPSCs) evoked by test stimuli at a low frequency (0.05 Hz) (*7*). For

Department of Biology, University of California at San Diego, La Jolla, CA 92093, USA.

*To whom correspondence should be addressed. E-mail: mpoo@ucsd.edu